出國報告（出國類別：其他）

大陸第二屆神經學與神經外科研討會出國報告

服務機關：核能研究所
姓名職稱：張剛瑋　副工程師
派赴國家：大陸
出國期間：104 年 12 月 17 日~104 年 12 月 21 日
報告日期：105 年 1 月 12 日

摘　　要

神經學與神經外科研討會議,主旨爲涵蓋腦中樞神經學影像與腦中樞治療問題，參與此會之人員包含：臨床醫師、神經學學者與神經外科學者等，此次會議約有百餘人參與。本計劃參加此會議,除了以海報方式分享本所先進的研究方法，並將投稿文獻以全文方式呈現，發表於；Journal of Biosciences and Medicines"（ISSN:2327-5081）期刊中，也期許藉參與會議獲得腦中樞診療最新技術應用發展及研發技術等資訊外，蒐集國外最新發展資料，激發新創意與構想，使本計畫實施策略更具彈性而具體。

關鍵字：神經學、神經外科

目　　次

（頁碼）

一、　目的

神經科學之研究起源於美國總統喬治布希於就任時，宣示自 1990 年至 1999 年爲腦的 10 年起至今已有將近 30 年的時間，其中由美國國家衛生院（NIH）主導，致力於神經科學研究，主要目的在研究腦細胞的發生與交互作用，以改善各項神經系統病變的治療。如今腦的 10 年已經結束，但神經科學研究正方興未艾，並持續邁入人類基因計畫時代，對於神經科學研究將更透徹。

現今的神經醫學面臨三大革命，一爲影像醫學的進步，電腦斷層掃瞄（MRI）核磁造影（NMR）與核醫診斷儀器（PET and SPECT）的發明，而可以直接看到頭顱內的病兆，二爲神經藥理學的建立，藉由神經傳導物質與受器的發現，來研究神經系統疾病的致病機轉與治療方向，三爲分子生物學的突破，探討疾病生成原因，對於遺傳性疾病可用產前分子遺傳診斷方式偵測，亦可針對部份疾病高危險群做早期預防與治療。

神經學，爲現今認知神經科學的重要理論應用之基礎。其整合神經科學之專業知能，與認知神經科學實驗的設計、執行，以及資料分析能力運用於現行行爲科學及生物醫學研究中。

神經外科是現代醫學亮眼的一科，如利用腦神經微創手術及脊椎功能保存手術。均有別於傳統神經外科手術在於以較少的侵入破壞，並減少手術併發症等。

本次公差之目的，爲參加大陸主辦的第二屆神經學與神經外科研討會議，會議於 2015 年 12/18～20 在大陸桂林市召開，會議中以神經學、神經外科等研究成果爲主。本計畫希望藉由該會議交換最新研究的成果、分享先進的研究方法、提供前瞻性研究交流討論爲目的。

二、 過程

(一) 行程：公差主要行程與內容如下表

表一、公差行程表

行程					公差地點		工作內容
月	日	星期	地點				
			出發	抵達			
12	17	四	台北	桂林			去程
12	18-20	五-日			大陸	桂林	2015 年神經學與神經外科研討會
12	21	一	桂林	台北			回程

(二) 公差歷程：

1. 12 月 17 日(週四)：台北（桃園機場）→大陸桂林

2. 12 月 18 日(週五)～20 日（日）：2015 年神經學與神經外科研討會

3. 12 月 21 日(週一)：大陸桂林→台北（桃園）

三、心　得

人腦研究從美國布希總統宣稱 20 世紀末是「大腦的十年」後，開始成爲顯學。2013 年 1 月，先是歐盟選定人腦計畫（Human Brain Project）爲「未來新興技術旗艦項目之一」，美國總統歐巴馬也在次月的國情咨文中將人腦計畫視爲「國家創新目標的一環」，隨後更宣布隔年將撥款一億美元投入「推進創新神經技術腦部研究」（Brain Research through Advancing Innovative Neurotechnologies, BRAIN）計畫，目標是透過腦造影等高科技技術繪製人腦圖譜，以了解大腦的運作機制，並由洛克斐勒大學和史丹福大學兩位神經科學家籌組「夢幻團隊」，先從了解大腦處理語言的運作開始，最終希望能夠找到治療癲癇、自閉症、精神分裂、阿茲海默症等複雜腦部疾病的新方法，這項計畫的意義被譽爲媲美 1990 年代的「人類基因組計畫」。

日本政府也因體認神經系統失調會產生諸多疾病的重要性，便把 21 世紀訂爲腦的世紀；相對的南韓也提出“Brain Korea 21（BK21）”計畫；中國大陸則針對 21 世紀之重點建設，選定 100 所高等學校和重點學科執行「985 計畫」與「221 工程」；香港也大力支持神經科學研究計畫。

相對的台灣聯合大學系統的中央大學認知神經科學研究所、陽明大學神經科學研究所，以及中央研究院腦磁波實驗室共同主辦的「2014 台灣認知神經科學暑期學校」，僅於會議中分享腦科學研究工具，以及介紹語言、注意力、記憶、認知老化等研究議題，相較之下，臺灣在這方面就略遜一籌。

演講內容：

（一）、德國柏林 Kerstin Hermelink 教授：Chemonbrain（化療腦）

Chemobrain（chemo fog）這一名詞，約 1997 年前後才出現，正式名稱爲認知功能障礙，是目前在許多癌症患者中經過化療後腦部會出現的症狀，大部分的研究來自於長期治療的女性乳癌患者，研究顯示不只有化學治療會影響病人的認知功能，包括放射治療、荷爾蒙治療、身體情緒（焦慮、沮喪等）、疲勞或老化，甚至於癌症本身皆可能影響病人的認知功能。據估計在所有癌症病人中，大約有 2～3 成的病人其神經認知功能會受到癌症本身或癌症相關治療影響，影響時間一般持續數週到數年之久，包含病人之情緒、人際關係、生活品質、職場生涯、社會功能及家庭生活。現今已可利用 functional MRI（fMRI）的研究確認病人的腦部功能的損傷。

1. 定義:

   輕微的認知異常(mild cognitive impairment)，常以記憶力減退，執行工作有困難或較不易學習新的技能來表現。

2. 原理：

   化療是目前針對癌症治療方式之一；針對大多數乳腺癌患者，再給予化療後，會涉及到一些腦部的副作用，稱爲：Chemobrain，當罹患 Chemobrain 時，會有難以有效地處理信息，又稱爲：化療腦。是由癌症患者描述癌症治療過程後（化療）可能出現的思維和記憶問題的常見詞，爲化療相關的認知缺損或認知功能障礙。

3. 症狀：

   (1). 遺忘東西，通常缺乏部分記憶（失憶）

   (2). 無法集中注意力

   (3). 遺忘：如姓名，日期，有時甚至較大型的活動很難記住細節

   (4). 需要較長時間才能完成的事情（雜亂無章，慢思考和處理）

   (5). 字彙減少（無法找到合適的語言來完成一個句子）

4. 改善方法

   (1). 用記事本，智慧型手機寫下重要事情，幫助提醒

(2). 動腦遊戲、拼圖、拼字、學新語言

(3). 足夠的睡眠和休息

(4). 規律的運動，每週 150 分鐘

(5). 多吃植物性食物（蔬食）獲取更多抗氧化植物素

(6). 建立生活常規模式，把易忘記的東西事情集中起來處理

(7). 一次作一件事情，不要一心多用

(8). 當身心很疲累時，調解你的腦力和體力，請家人親友幫忙

(9). 瑜珈、太極拳、靜坐冥想等身心紓壓方法緩解憂鬱焦慮情緒

(10). 輕鬆心情面對，有時候的記憶力差或是專注力問題，不用太計較或在乎這問題的多寡，給自己一些時間和空間,會慢慢改善的

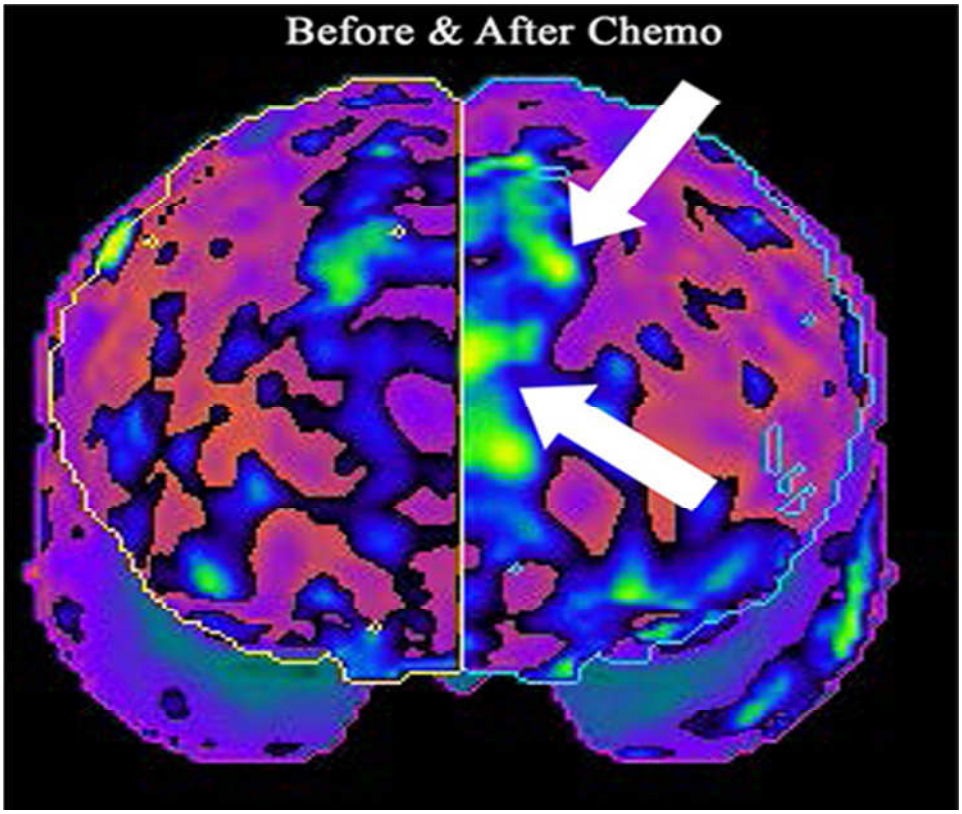

圖一、試驗證明於化療後腦部 fMRI 影像差異性（By: http://breastcancerhealingmoments.blogspot.tw/2015/03/chemo-brain.html）

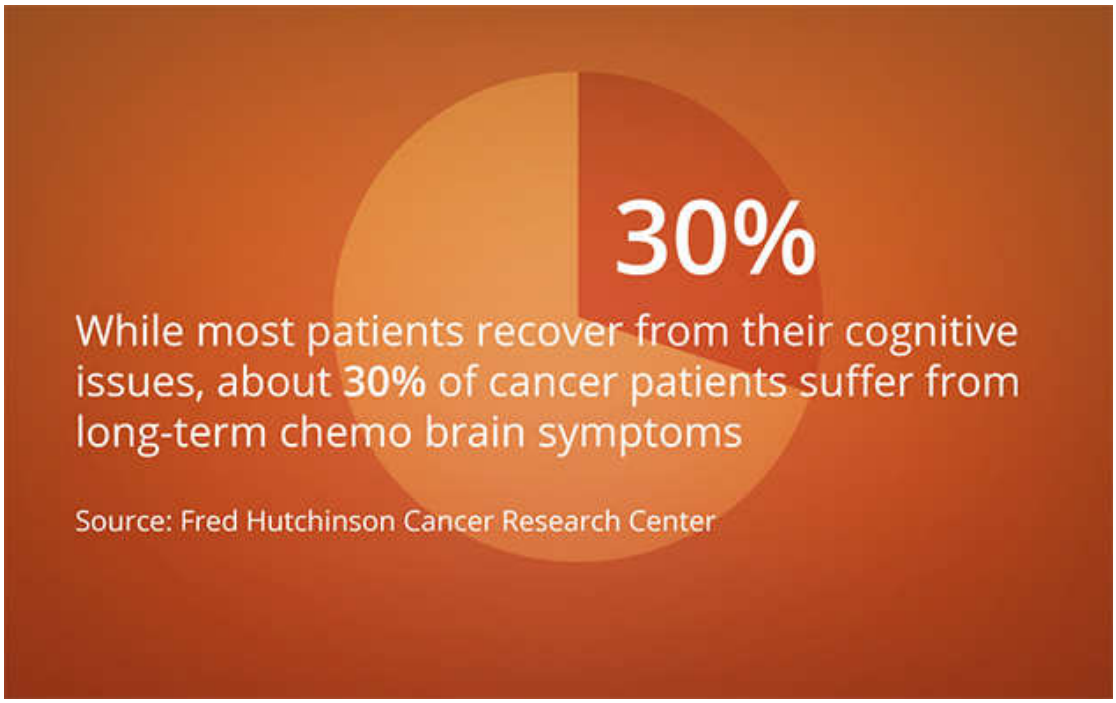

圖二、依據統計，有 30%的化療治療患者將有 ChemBrain 的症狀（By: http://blog.stmarkshospital.com/blog/2015/06/11/coping-with-chemo-brain-during-cancer-treatment/）

5. 本所研究相關性：

現今由於化學藥物針對癌症病患的治療效果，因而導致腦部出現變異性的癥狀，目前於會議中並無法改變現有的醫療體系。由於醫師用藥與癌病患者的要求，使用化療方式仍爲醫師首要運用方式。且在化療藥物進行相關臨床性試驗前，均會針對人體主要器官、組織、血液等系統進行安全評估作業，相對而言應爲安全使用劑量。

本所研發腦部相關核醫診斷藥物已有將近 20 年時間，期間發展 DAT、SERT、D2 等多樣的核醫診斷藥物，使用藥物的用量均爲 tracer level，現今尚未發現有任何影響腦部的報告產生；未來本所發展類似藥物，腦部相關病變的發展，也將是需要注意的地方。

其次，核醫醫學影像技術即在於進行活體即時的診斷方式，現今針對 ChemBrain 的診斷方式大多使用 fMRI，但核醫影像的 PET、SPECT 搭配神經系統診斷藥物，將有助於醫師了解藥品影響腦部發展的關鍵，這也是作爲醫療行爲第二線的核醫系統，應發展的角色。

（二）、美國邁阿密 Mary Bartlett Bunge 教授：Study finds axon regeneration after Schwann cell graft to injured spinal cord（新三合一療法於許旺氏細胞移植）

1. 美國邁阿密計畫的科學家以一種新的三合一綜合療法可讓癱瘓老鼠恢復了 70% 的行走能力，被視爲是脊髓受損研究的一項突破。

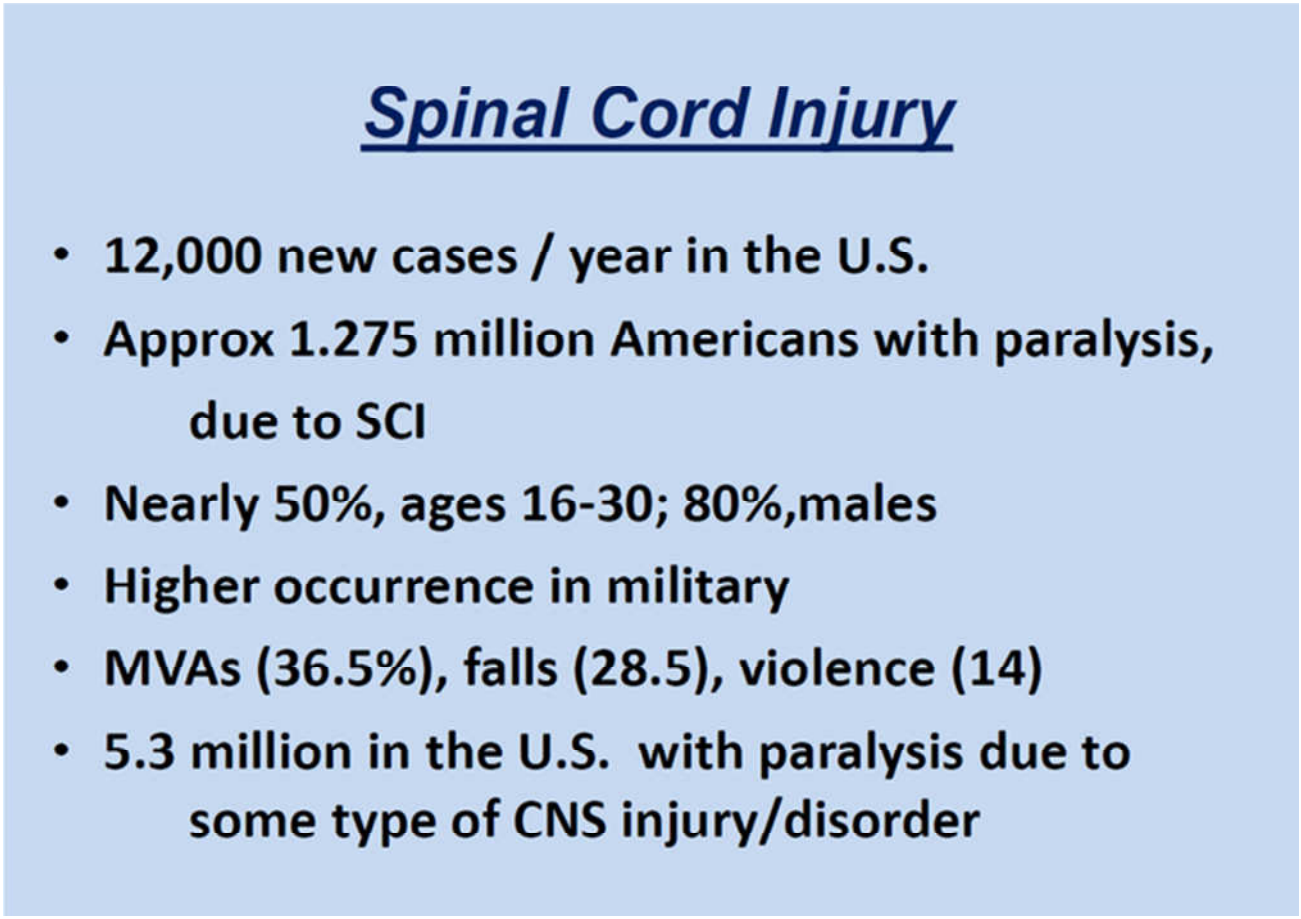

圖三、研究統計現今每年在脊髓傷害在美國的罹患率

表二、脊髓傷害於不同年齡層與評估社會資源使用量

Severity of Injury	Aver Yearly Expenses (Feb 2013)		Est Lifetime Costs Age at Injury	
	First Year	Each Subsequent Year	25 years old	50 years old
High Tetraplegia (C1 –C4)	$1,044,197	$181,328	$4,633,137	$2,546,294
Low Tetraplegia (C5-C8)	$754,524	$111,237	$3,385,259	$2,082,237
Paraplegia	$508,904	$67,415	$2,265,584	$1,486,835

2. 脊髓有很多神經細胞網路，負責在腦部和肌肉間傳遞訊息。脊髓受傷時，神經細胞網路遭切斷，導致癱瘓。通常，體內的化學訊號會阻上神經細胞再生。如何讓神經細胞再生、把它們重新銜接起來，一直是脊髓研究科學家所追求的「聖杯」。
3. Dr. Mary Bunge 一生致力於許旺氏細胞移植 (Schwann cell grafts) 治療脊髓損傷的研究，並成功發展許旺氏細胞在體外培植、增生的技術。不過，能在周邊神經產生再生功能的許旺氏細胞移植到中樞神經後，卻被抑制不能發生作用。

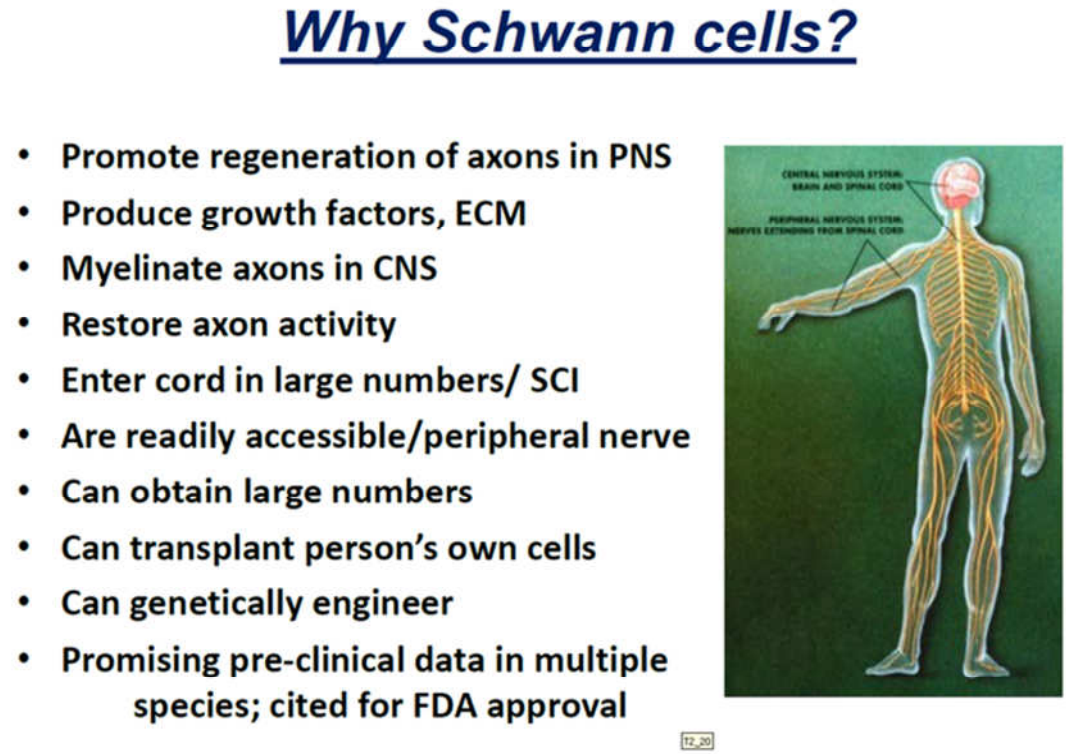

圖四、許旺氏細胞作爲修復脊髓傷害之優點圖

4. 研究人員把末稍神經的鞘膜細胞（又稱許旺氏細胞）移植到脊髓受傷部位，刺激傳遞訊息的神經軸突的再生，重建細胞間的橋樑。鞘膜細胞也可製造髓鞘質，隔離保護神經纖維。先前研究發現，移植鞘膜細胞可促進脊髓受傷部位新神經纖維的再生，但很快就停止了。

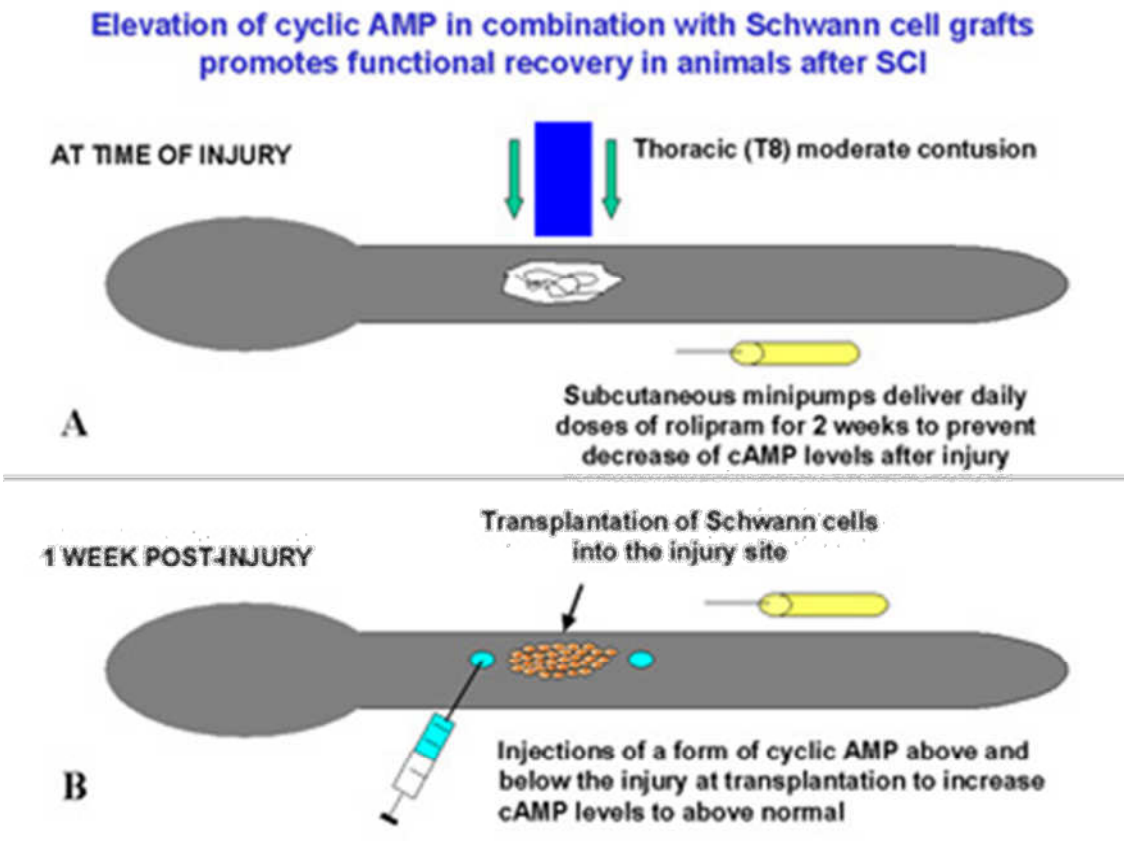

圖五、許旺氏細胞合併環核甘酸（cAMP）治療脊髓傷害示意圖

5. Dr. Bunge 採取複合療法，把這種許旺氏細胞移植法與另兩種療法併用，第一個療法是注射抗抑制藥物---環核甘酸（cyclic AMP, 簡稱 cAMP），環核甘酸是導引神經細胞長出銜接纖維的信息份子， cAMP 可在神經細胞受抑制的環境中，引導軸突成長；另一療法是注射預防環核甘酸分解的藥物 Rolipram 。
6. 研究進行八週後，未接受治療的老鼠雖可斷斷續續地走，但無法一步接一步的走。接受治療的老鼠則恢復了 70% 的行走能力，是「頗顯著的進展」，牠們可持續地走，行動控制和協調能力也都較佳。

   不僅如此，治療組的老鼠身上的組織也較多，顯示這似可避免一般脊髓受傷者通常會出現的二度組織喪失情形。治療組老鼠移植細胞部位神經纖維增加了五倍。

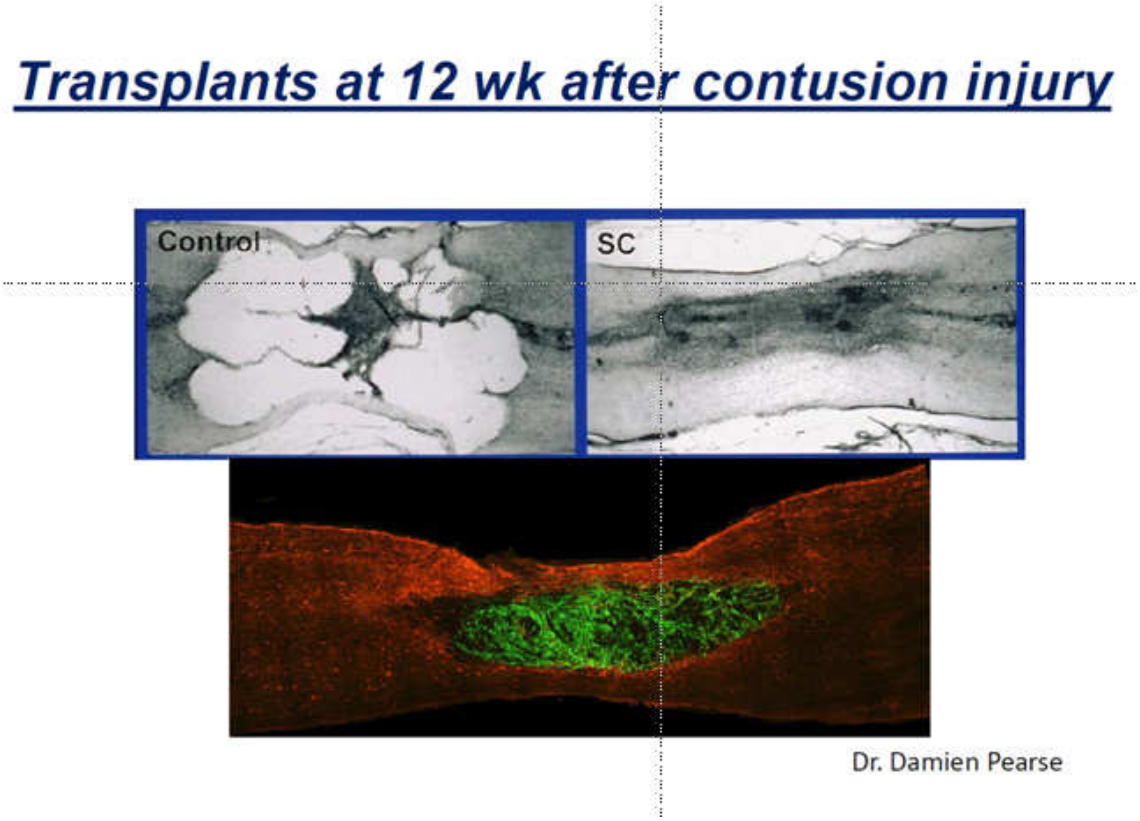

圖六、治療 12 週後脊髓切面圖

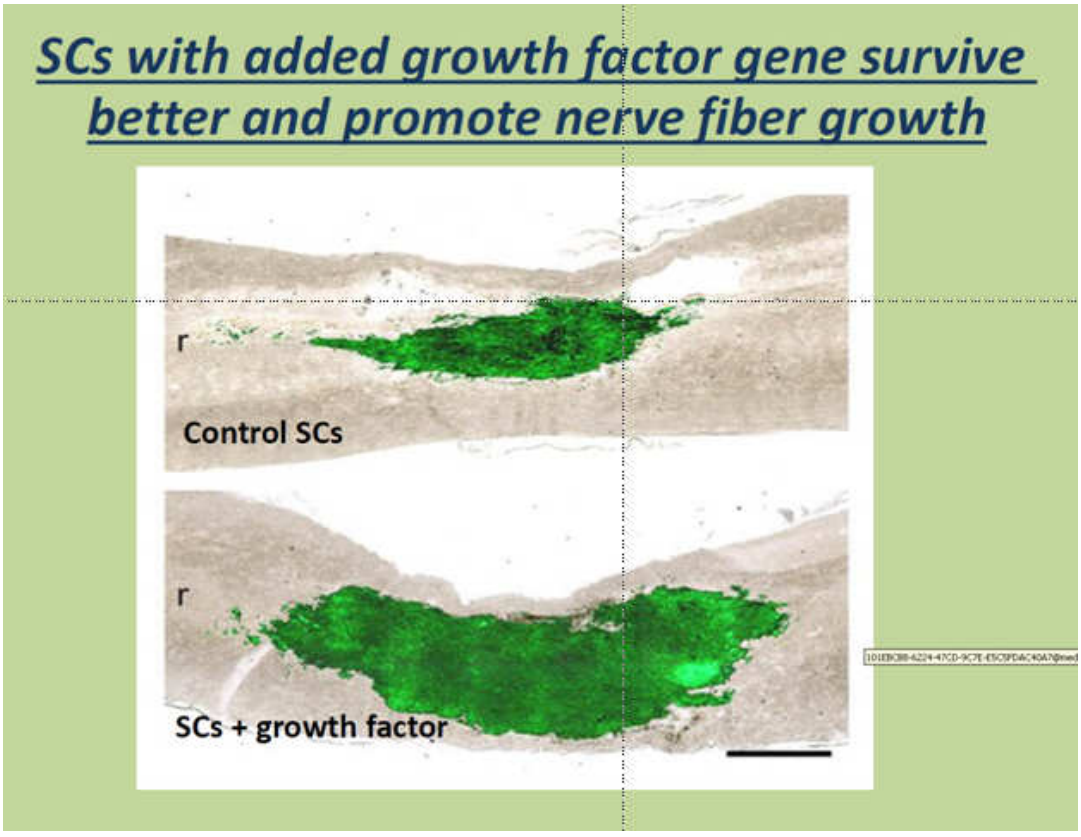

圖七、許旺氏細胞合併生長激素治療後脊髓切面圖

7. 本所研究相關性：

本次會議除了神經學外，也廣邀神經外科的學者發表演說，此篇即是利用許旺氏細胞作爲治療脊髓的研究發展。目前在美國脊髓（柱）傷害的罹患率與造成美國經濟的負擔是日漸增多，且經流行病學的統計，大都均爲 16-30 歲年輕的男性，且越年輕罹患將造成社會的負擔越大。該報告者利用許旺氏細胞鞘膜細胞可刺激、傳遞訊息的神經軸突合併環核甘酸（cAMP）移植到脊髓受傷部位，重建脊髓傷害細胞間的再生，作爲治療的方式。

現今除了神經外科的治療方式，也有利用幹細胞治療帕金森氏症腦部病變的方式，均在利用一些外在方式，給予腦部神經再生、活化等治療。本所過去發展腦部影像整合系統，即在於將疾病動物模式，進行各種神經核醫影像醫學的處理方式，用以達到各樣疾病的腦部影像結果，以便用于未來治療藥物的篩選或是治療後之療效評估。本所發展的 Tc-99m-TRODAT-1 神經診斷藥物，即利用於帕金森氏症的治療藥物篩選工作，顯示本所作爲醫療系統的輔助角色，確有其存在的必要性。

（三）、大陸山東大學陳哲宇教授：：Wnt3a 參與海馬依賴的記憶形成

1. Wnt 蛋白是一種分子量爲 39-46KD 的分泌型糖蛋白，當分泌到胞外的 Wnt 分子與細胞膜上 Frizzled 受體結合後能引起細胞內一系列信號通路的啓動、 包括 Wnt/β-catenin、 Wnt/Ca2 + 和 Wnt/PCP 通路。

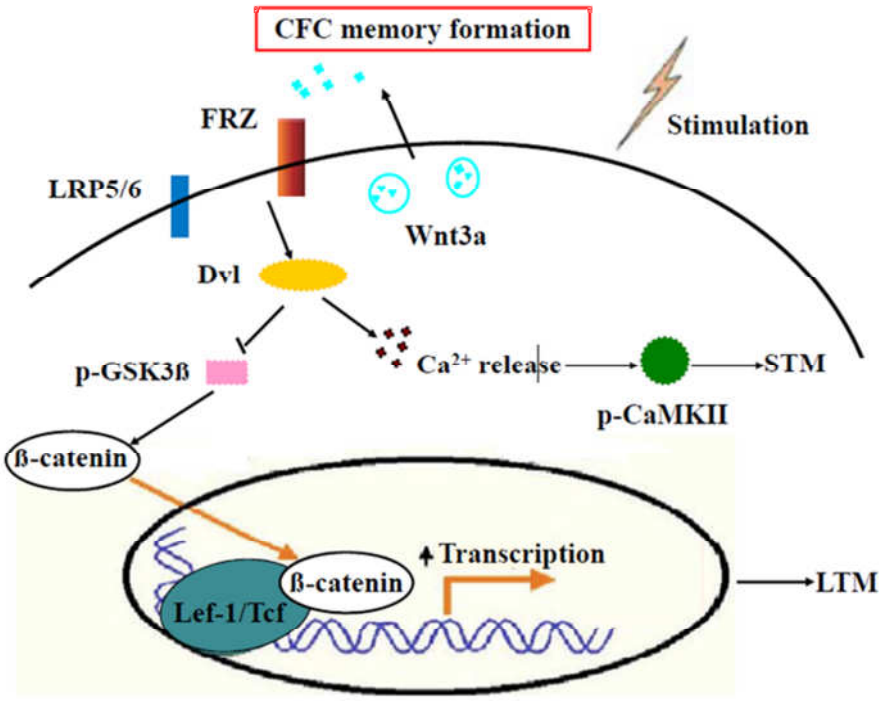

CFC 训练诱导海马脑区 Wnt3a 分泌及表达升高；释放到胞外的 Wnt3a 通过与其受体结合激活下游的 Wnt/Ca^{2+}与 Wnt/β-catenin 信号通路，分别调控 CFC 记忆的获得与整合。

圖八、Wnt 蛋白作用於記憶傳導示意圖

2. 根據 Wnt 信號通路的不同將 Wrnt 蛋白分爲兩大類即經典 Wnt 蛋白和非經典 Wnt 蛋白。Wnt 受體及其信號通路中 a 的相關組成在神經系統中有廣泛分佈。研究顯示，Wnt 信號通路在神經發育過程中發揮重要作用，如海馬迴的形成，神經樹突形態構建，軸突導向以及突觸形成等。近年來 Wnt 在成熟中樞神經系統中的作用也越來越受到人們的關注，研究發現 Wnts 在成熟中樞神經系統突觸可塑性的調控以及成年動物的學習記憶過程中發揮著重要作用。
3. 動物實驗顯示：條件性恐懼記憶訓練後，小鼠杏仁體腦區中的 Wnt1 mRNA 出現了顯著性下降；若是於訓練前在小鼠杏仁體腦區注射 Wnt1 蛋白能引起小鼠長時間記憶的損傷。Wnts

及其信號通路相關組分在神經系統中有廣泛分佈，但是現今哪個 Wnt 分子參與海馬迴依賴的學習記憶尚不清楚，Wnt 介導的不同信號通路在學習記憶中的功能有何異同也不明確。

4. 本次會議作者提出：

(1). 針對海馬迴依賴的恐懼記憶作爲實驗模型，研究成年小鼠海馬迴腦區中 Wnt 調控學習記憶的作用及其機制。研究顯示，恐懼記憶方式（CFC 訓練）首先誘導 Wnt3a 的快速釋放，進而正回饋促進 Wnt3a 的合成增加，並且能啓動 Wnt3a 下游 Wnt/Ca2 +與 Wnt/β-catenin 信號通路。表明 Wnt3a 是 CFC 記憶形成的必要且充分條件。

(2). 探討動物腦區給予外源性 Wnt3a 增強 Wnt3a 信號促進 CFC 記憶的形成：在海馬腦區注射 Wnt3a 中和抗體（sFRP1 抑制劑）阻斷 Wnt3a 信號可以抑制 CFC 記憶的形成在海馬腦區注射 Wnt，此信號通路可以阻斷 CFC 的短時記憶與長時記憶，而注射經典 Wnt 信號通路抑制劑（DKK1）則只阻斷長時記憶而對短時記憶沒有影響，表明 Wnt/Ca2 +與 Wnt/β-catenin 信號通路分別參與 CFC 記憶的獲得與整合。

5. 本所研究相關性：

神經醫學利用核磁共振影像成像技術（如 CT、MRI）期望以非侵入性的檢測方式針對腦部發生病變的位置進行初步的定量，但目前尚有困難（如：腦部區域的高解析度掃描工作需過久的時間或是疾病的治病原因至今仍不完全了解）。利用 PET 與 SPECT，可發展針對核醫分子影像醫學技術進行功能性的檢測，提供於腦部的治療療效評估。結合不同影像系統架構，如結合 PET 影像和核磁共振影像（高解析度）將可增加對於體內的對比解析度分析，詳盡的描繪生理過程和結構，成爲藥物開發階段的關鍵元素。

本次報告學者利用分子層面探討恐懼記憶的動物模型對於記憶時間的長、短，蛋白質 Wnt 參與的量有多少，分子層面的探討是目前本所未曾涉獵的部份；本所研發在於建立完整的核醫影像造影劑，未來應當擷取基礎研究的報告（如分子層面的探討），由其中找尋爲來合適藥物的發展，因爲客製化的核醫藥物將會是未來的趨勢，針對不同疾病、患者的診斷、治療方式將有所差異，故未來若要發展分子、蛋白質等核醫藥物，更應多涉獵類似報告。

（四）、中國上海鮑嵐研究員： CaMKII 和 caveolin-1 協同調控 ATP 誘導 P2X3 受體

1. ATP 藉由離子通道（P2X3、P2X2）受體之選擇性，對於初級感覺神經元對生理性、病理性痛覺的調節至關重要。其中 P2X3 受體的合成、組裝和轉運對於其行使正常的功能是必需的。研究指出，若是大量釋放的包括 ATP 在內的各種癌症因數多與 P2X3 受體的調節能力有關。於此研究中，發現 ATP 可以促進 P2X3 受體的內吞、進而形成信號內吞體、 在初級感覺神經元軸突中逆向轉運到胞體、 活化轉錄因數 CREB、調節神經元的興奮性。但是 ATP 對 P2X3 受體上膜轉運的調節及機制仍不清楚。

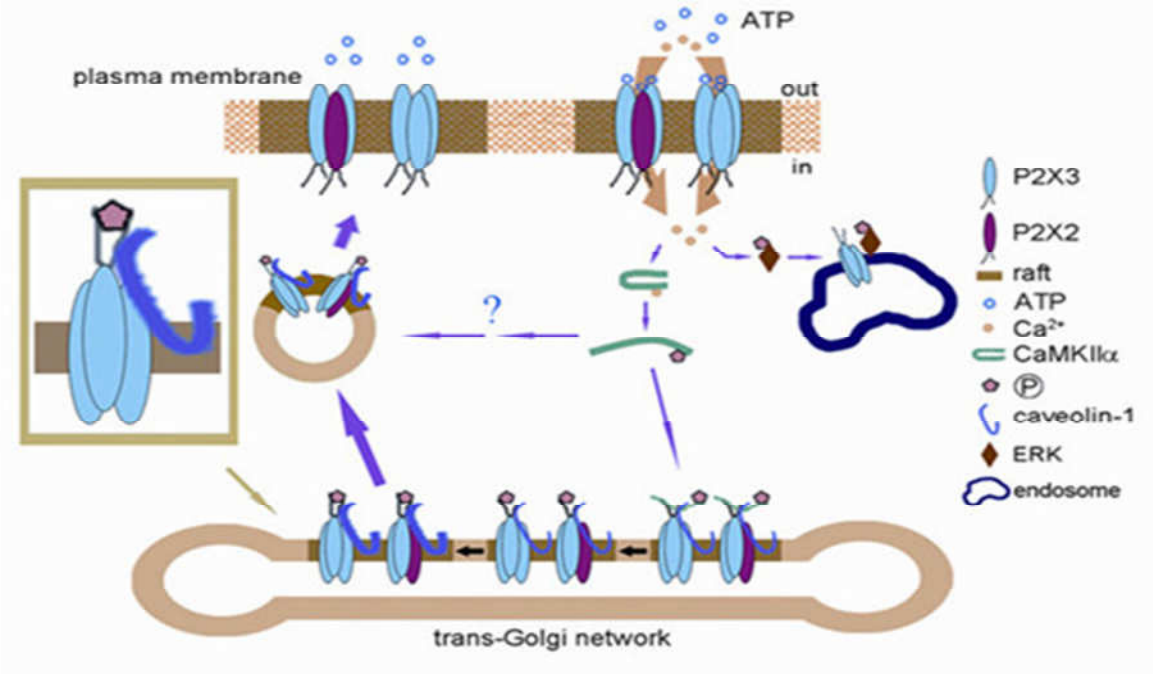

圖九、ATP 藉由 P2X3、P2X2 通道，傳遞神經訊號示意圖

2. 本次會議作者提出：

(1). ATP 給予時間的不同可造成背根神經元中內源性的 P2X3 受體的上膜轉運，而同家族的 P2X1 和 P2X2 受體則沒有此效應。顯示 ATP 可啓動 P2X3 受體引起的鈣離子內流，並且可以啓動鈣/調節 P2X3 受體的上膜轉運。

(2). CaMKII α 蛋白經由鈣調素（Ca）調節，並作用於依賴性蛋白激酶 II α P2X3 受體的 N 端，而位於其 C 端的第 388 位蘇氨酸 (Thr388) 可被 CaMKII α 磷酸化。進一步研究發現，脂筏結構的組成蛋白 caveolin 1 能與 P2X3 受體相互作用，通過基因抑制 caveolin-1 的表達

或者消除 P2X3 受體結合 caveolin-1 的能力均可抑制 ATP 依賴的 P2X3 受體的上膜轉運。此項研究爲痛覺傳遞中 P2X3 受體的功能調控提供了一種可能的機制。

3. 本所研究相關性：

癌症藉由 ATP 通道的通透性增加與癌症病程的相關研究，已有非常多文獻發表。現今針對 ATP 通道的調控機制，如：CaMKII 和 caveolin-1，來協同調控 ATP 的機轉爲本次報告者之主題。

CaMKII：伏隔核（Nucleus Accumbens）是大腦中掌管快樂、恐懼、成癮等重要作用的中樞，古柯鹼會刺激伏隔核中的細胞，增加兩種蛋白質的產量，其中一個就是與學習有關的 CaMKII。CaMKII 的大量表現將會讓動物即使在沒有吸毒的情況下，仍然表現出和吸毒時一樣的行爲。Caveolin-1（Cav—1）蛋白：該蛋白在膽固醇運輸、細胞膜組裝、神經信號傳遞過程中扮演重要的角色。

現今本所在神經醫學方面，主要探討阿茲海默氏症（Alzheimer’ s disease, AD）與帕金森氏症（Parkinson syndrome, PD），其中的學習、記憶與藥物成癮等的確與 ATP 的傳導機制有相關作用。

若要以分子機制的層面來看核醫藥物，這不是核醫影像醫學該進行的部份，核醫本是用巨觀的看法來評估單一癥狀的差異性，若僅就某一分子層面就顯得有些狹隘；但科技日新月異，或許有朝一日將會是分子影像的世界，屆時針對分子層面的核醫定量或許就是客製化醫療最終會達到的目標。

（五）、結論：

神經學與神經外科研討會議，主旨爲涵蓋腦中樞神經學影像與腦中樞治療問題，該會議以交換最新研究的成果、分享先進的研究方法、提供前瞻性研究交流討論的國際平台爲目標。綜合參加此會議，可以掌握目前國際腦中樞藥物開發之脈動。希望藉由與學者之密切交流與學習，激發新創意與構想，以及後續計畫之推動。

本次會議之目的：

1. 發表論文，提升本所國際知名度。

2. 與來自世界各國、不同領域之專家與會，藉參與會議獲得腦中樞診療最新技術應用發展及研發技術等資訊。

四、建議事項

（一）參加第二屆神經學與神經外科研討會議心得如后：本次研討會共邀請美國、德國、日本、印度等各界學者發表論文。本所爲第一次奉派參與此會，藉機獲得國際間神經學與神經外科領域之最新發展，未來應多參與類似會議。

（二）此次會議主要題目在於：1. Chembarin：經由化療治療乳癌的患者，在多年後均可發現在腦部記憶、行爲與表現上，呈現腦部傷害之跡象。且由 fMRI 的輔助診斷也可發現腦部出現異常，顯示過去在於化療藥物的開發過程中，缺乏影像醫學部分，這也是這幾年核醫分子影像醫學獲得重視的原因之一。2. Schwann cell（許旺氏細胞）治療脊髓病患：利用許旺氏細胞作爲治療脊髓患者，加速其恢復健康，也是神經外科現今在努力發展的方向。本所研發工作針對神經科學與神經外科，應與世界接軌之研發工作。

（三）本次會議雖由大陸神經學與神經外科學會主辦，但於 會議中敬邀多位 SCI 雜誌的負責人或 Editor 作爲座長，於會議中敬邀與會學者投稿，除了此次會議本身摘錄全文於 Journal of Biosciences and Medicines 外，也有其他領域文獻在與會中邀稿，針對學術方面並不設限於單一學術領域。本所同仁可藉由參與類似會議得到文獻發表之機會，藉機彰顯本所研究成果。

（四）神經科學相對於生物學領域，是現今比較新興的學門，大概在第二次世界大戰後（約 1950 年）才逐漸興起。近幾十年來常聽到的精神病、憂鬱症、老年癡呆症等，都屬於神經科學的範圍。在世界各國均大量投資經費研究的相較之下，本所著力於腦中樞神經研究工作相對就格外重要。\

五、附錄

1. 投稿論文摘要

Abstract:

Purpose: 2-(1-{6-[(2-[18F]-Fluoroethyl)(methyl)amino]-2-naphthyl}ethylidene) malononitrile ([18F]-FDDNP) was synthesized and characterized as a positron-emitting probe to identify Alzheimer’ s disease (AD) in transgenic mouse models (Tg2576 and dE9) expressing the AD pathology. We observed in in vitro, in vivo, and ex vivo studies that [18F]-FDDNP accumulated specifically in the Aβ-overexpressing brain regions and that this accumulation was significantly reduced by co-incubation with non-radioactive FDDNP.

Methods: The [18F]-FDDNP was undergone evaluated by studying its in vitro competition, ex vivo autoradiography and in vivo microPET image with three strains (Tg2576, dE9 and normal mice). These assays will receive [18F]-FDDNP and assessment of the area of interest regions were performed on tissue slices. ELISA assay will assess with different regions of the brain with human amyloid β (1 – 40) protein quantity.

Results: In ex vivo and in vivo studies of brain sections, the retention of radioactivity was more specific in Tg2576 mice than in dE9 mice. Quantification of human amyloid β (1 – 40) showed that the Tg2576 mice had significantly higher levels than the dE9 or normal mice in whole brain regions. Using in vitro, ex vivo, in vivo, and Enzyme-linked immunosorbent assay (ELISA) analyses, we characterized the utility of [18F]-FDDNP in mapping -amyloid in the Tg2576 mouse brain, to assess its potential application in imaging strategies.

Conclusions: This study demonstrates that the application of [18F]-FDDNP combined with Tg2576 mouse may be useful for monitoring the formation and progression of Aβ in the brain, for extrapolation to AD patients.

Keywords [18F]-FDDNP · Alzheimer’ s disease · Transgenic mice · β-Amyloid plaques

2. 大會會議地點、時間

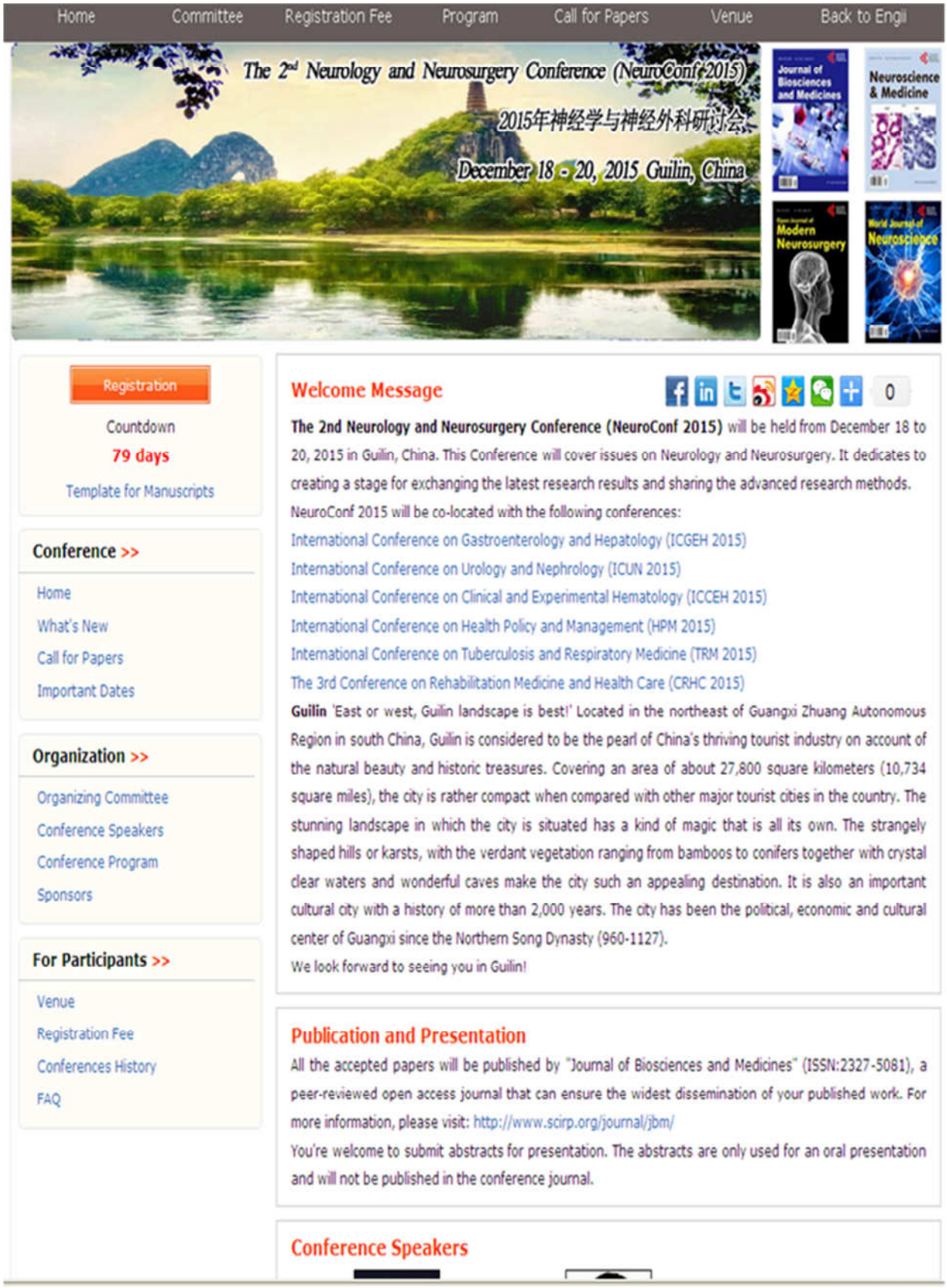
Home
Committee
Registration Fee
Program
Call for Papers
Venue
Back to Engli
The 2nd Neurology and Neurosurgery Conference (NeuroConf 2015)
2015年神经学与神经外科研讨会
December 18 - 20, 2015 Guilin, China
Registration
Countdown
79 days
Template for Manuscripts
Conference >>
Home
What's New
Call for Papers
Important Dates
Organization >>
Organizing Committee
Conference Speakers
Conference Program
Sponsors
For Participants >>
Venue
Registration Fee
Conferences History
FAQ
Welcome Message
0
The 2nd Neurology and Neurosurgery Conference (NeuroConf 2015) will be held from December 18 to 20, 2015 in Guilin, China. This Conference will cover issues on Neurology and Neurosurgery. It dedicates to creating a stage for exchanging the latest research results and sharing the advanced research methods.
NeuroConf 2015 will be co-located with the following conferences:
International Conference on Gastroenterology and Hepatology (ICGEH 2015)
International Conference on Urology and Nephrology (ICUN 2015)
International Conference on Clinical and Experimental Hematology (ICCEH 2015)
International Conference on Health Policy and Management (HPM 2015)
International Conference on Tuberculosis and Respiratory Medicine (TRM 2015)
The 3rd Conference on Rehabilitation Medicine and Health Care (CRHC 2015)
Guilin 'East or west, Guilin landscape is best!' Located in the northeast of Guangxi Zhuang Autonomous Region in south China, Guilin is considered to be the pearl of China's thriving tourist industry on account of the natural beauty and historic treasures. Covering an area of about 27,800 square kilometers (10,734 square miles), the city is rather compact when compared with other major tourist cities in the country. The stunning landscape in which the city is situated has a kind of magic that is all its own. The strangely shaped hills or karsts, with the verdant vegetation ranging from bamboos to conifers together with crystal clear waters and wonderful caves make the city such an appealing destination. It is also an important cultural city with a history of more than 2,000 years. The city has been the political, economic and cultural center of Guangxi since the Northern Song Dynasty (960-1127).
We look forward to seeing you in Guilin!
Publication and Presentation
All the accepted papers will be published by "Journal of Biosciences and Medicines" (ISSN:2327-5081), a peer-reviewed open access journal that can ensure the widest dissemination of your published work. For more information, please visit: http://www.scirp.org/journal/jbm/
You're welcome to submit abstracts for presentation. The abstracts are only used for an oral presentation and will not be published in the conference journal.
Conference Speakers

3. 論文接受函

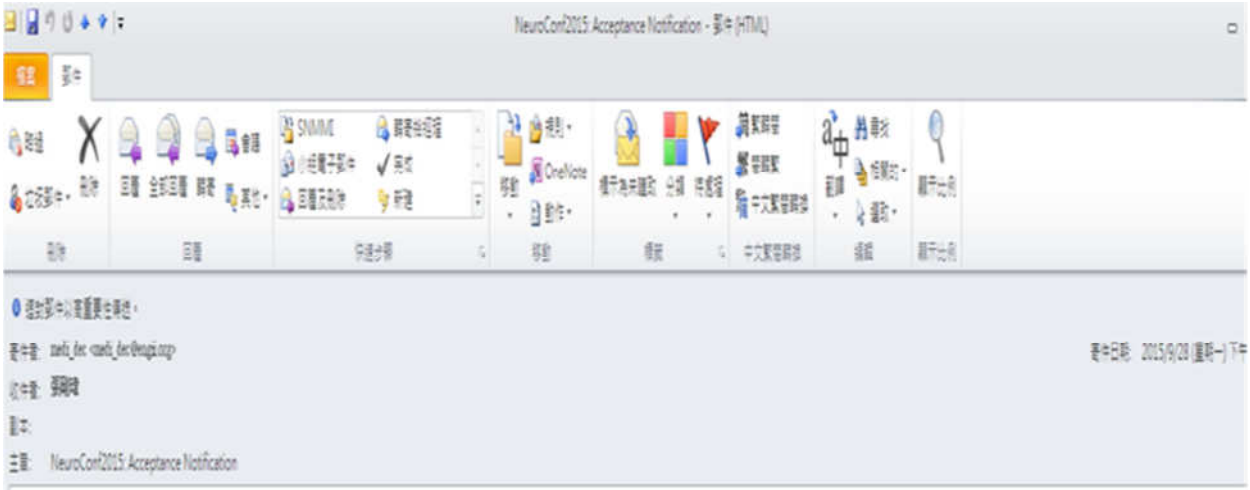

Dear Author,

Thanks for your paper submission!
We are pleased to inform you that your paper:
ID: NeuroConf2015Dec_604
Title: Transgenic mouse (Tg2576) is an ideal model for the biological characterization of [18F]-FDDNP (2-(1-(6-[(2-[18F]-fluoroethyl)(methyl)amino]-2-naphthyl)ethylidene)malononitrile) for identifying Alzhei
has been accepted for the final program.

You can finish the three steps below before October 10, 2015.
Step 1: Making Registration Payment
Step 2: Uploading Your Paper and Submitting Your Copyright
Step 3: Providing Registration Information

Please login to http://www.engii.org/papersubmission/default.aspx?ConferenceID=141 with your username and password; you can get more information under the column of "Registration Instructions".

For abstract submission, please note:
You only need to finish the Step 1 and Step 3.
Only full papers can be published. The abstracts will be presented in the conference.

We are looking forward to seeing you in Guilin, China!

Best Regards,
Rolin
Email: medi_dec@engii.org
Tel: 151 7247 9625
QQ: 3025797047
Organizing Committee

==========

This message has been analyzed by Deep Discovery Email Inspector.

4. 壁報張貼

Transgenic mouse (Tg2576) is an ideal model for the biological characterization of [18F]-FDDNP for identifying Alzheimer's disease

Kang-Wei Chang, Shih-Ying Lee, Chia-Chieh Chen

Division of Isotope Application, Institute of Nuclear Energy Research, Taiwan

Object

[^{18}F]-FDDNP was synthesized and characterized as a positron-emitting probe to identify Alzheimer's disease (AD) in transgenic mouse models (Tg2576 and dE9) expressing the AD pathology. We observed in in vitro, in vivo, and ex vivo studies that [^{18}F]-FDDNP accumulated specifically in the Aβ-overexpressing brain regions and that this accumulation was significantly reduced by co-incubation with non-radioactive FDDNP. In ex vivo and in vivo studies of brain sections, the retention of radioactivity was more specific in Tg2576 mice than in dE9 mice. Using in vitro, ex vivo, in vivo, and ELISA analyses, we characterized the utility of [^{18}F]-FDDNP in mapping β-amyloid in the Tg2576 mouse brain, to assess its potential application in imaging strategies.

Methods

Nuclear Medicine Research (instrument)

Auto-synthesizer for F-18-FDDNP

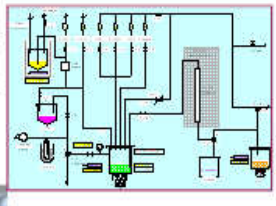

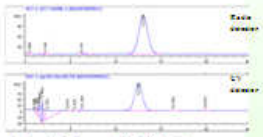

Identify by radio-HPLC

F-18-FDDNP log P = 1.93 ± 0.10

Analytic instrument

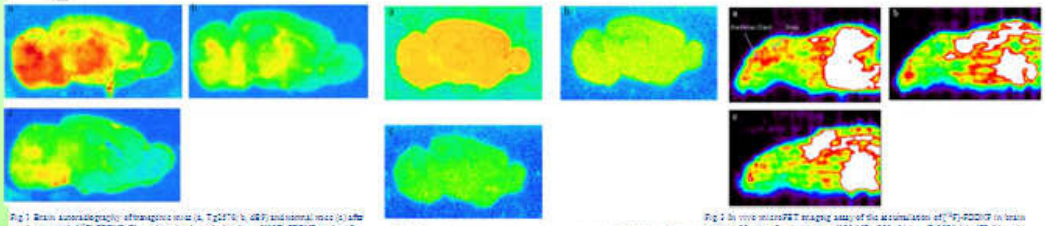

Fig 1 Brain autoradiography of transgenic mice (a, Tg2576; b, dE9) and normal mice (c) after incubation with [^{18}F]-FDDNP. The a, b, and c show the binding of [18F]-FDDNP to the Aβ-rich regions in brain sections.

Fig 2 Ex vivo brain autoradiography of transgenic mice (a, Tg2576; b, dE9) and normal mice (c) 30 min after injection with 185 MBq 200 μL [^{18}F]-FDDNP.

Fig 3 In vivo microPET imaging assay of the accumulation of [^{18}F]-FDDNP in brain sections 30 min after its injection (185 MBq 200 μL) into Tg2576 (a), dE9 (b), and normal mice (c). The arrows indicate the relative position of the brain (brain regions and Harderian glands). The transaxial microPET images clearly show that the uptake of [^{18}F]-FDDNP differs in the transgenic and control mice.

1. The results of in vitro autoradiography and a competition assay (Fig. 1) demonstrate the high binding capacity and specificity of FDDNP in the Tg2576 transgenic mouse. In the Aβ-rich brain regions (hippocampus and frontal cortex), the dE9 mice also displayed significantly higher binding than the normal mice ($p<0.01$), whereas the Tg2576 mice displayed significantly higher binding than the dE9 and normal mice in all the brain regions. Immuno-histochemical staining of the Tg2576 mouse brains also identified high levels of Aβ protein in the hippocampus and frontal cortex (data not shown).
2. Ex vivo autoradiography was also used to compare the binding of [^{18}F]FDDNP to the Aβ-rich regions in the transgenic and normal mice (Fig. 2). The Tg2576 mice showed significant differences from the dE9 mice in the binding of [^{18}F]FDDNP in the thalamus, midbrain, and medulla, and significant differences from the normal mice in the thalamus, midbrain, medulla, and cerebellum. [^{18}F]FDDNP binding differed significantly between the dE9 and normal mice in the midbrain, medulla, and cerebellum. In this assay, whole-brain sections from the Tg2576, dE9, and normal mice were assessed and compared.
3. MicroPET imaging was performed 30 min after the injection of [^{18}F]FDDNP (18.5 MBq). The specific binding ratios in whole brain regions showed greater accumulation of [^{18}F]FDDNP in the Tg2576 mice than in the dE9 or normal mice (Fig.3). In the past, the resolution and sensitivity of the imaging tools have not been rigorously considered in studies of brain radiopharmaceuticals. Klunk et al. [20] used [18F]-FDDNP/microPET (Siemens microPET Focus 220) to examine Tg2576 and control mice.

Conclusions

The present study suggests that [^{18}F]FDDNP has excellent potential utility in Tg2576 mice, but not in dE9 mice, and that this correlates with the amounts of Aβ protein in their brains.

2015. December. 18-20

行政院原子能委員會核能研究所

5. 期刊發表

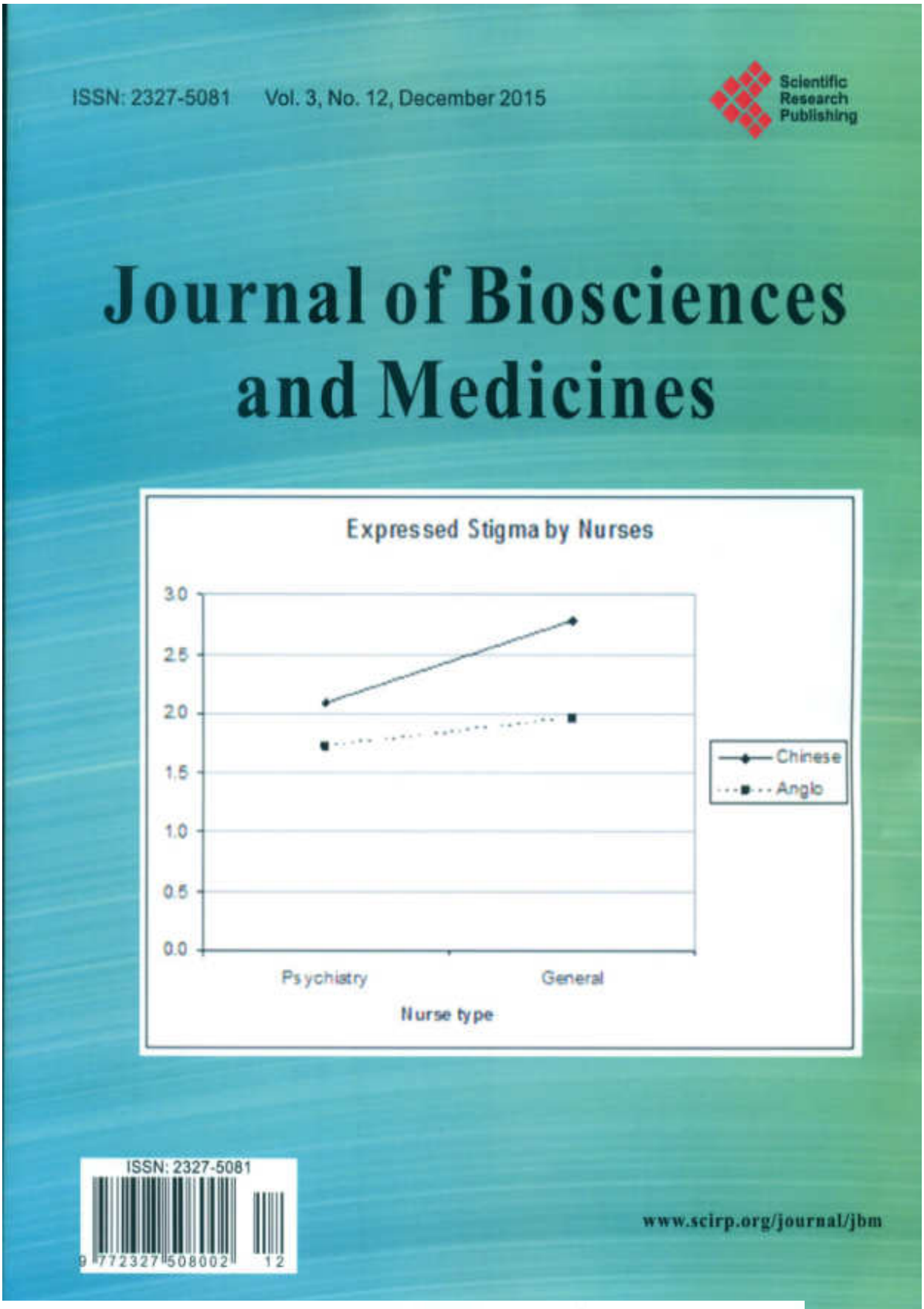

Journal of Biosciences and Medicines, 2015, 3, 1-6
Published Online December 2015 in SciRes. http://www.scirp.org/journal/jbm
http://dx.doi.org/10.4236/jbm.2015.312001

Scientific Research Publishing

AD patients for PET analysis [1] [2].

Laboratory animals with a marker of the disease are very useful in determining the pathogenesis of AD and identifying promising treatments [7]. Numerous models have successfully replicated amyloid plaque deposition and the inclusion of a mutant presenilin (*PSEN1*) allele can accelerate the deposition rate and exacerbate the pathological severity of the disease [1] [8].

To further characterize the binding properties of [^{18}F]-FDDNP in transgenic rodents, we extended APP transgenic mouse (Tg2576) and the PS/APP double-transgenic mouse (dE9), which express AD. The results of our studies of [^{18}F]-FDDNP used *in vitro* and *ex vivo* and with microPET imaging to predict the pathogenic processes of AD and provide a standard diagnostic method for this disease.

2. Materials and Methods

2.1. Chemicals

The precursor of FDDNP was purchased from ABX (Radeberg, Germany). Acetic anhydride, 30% hydrogen peroxide, potassium iodide, dimethyl sulfoxide, potassium carbonate, ethylene glycol, anhydrous acetonitrile were purchased from Merck & Co., Inc. (Whitehouse Station, NJ, USA).

2.2. Animal Models

14 - 16-month-old transgenic Tg2576 and dE9 mice expressing mutated human APP and APP/PS1 proteins, respectively. All animal procedures and experimental protocols were approved by the Ethical Animal Use Committee of the Institute of Nuclear Energy Research (INER), Taiwan.

2.3. Synthesis of [^{18}F]-FDDNP

FDDNP was prepared according to the procedure published in 2007 [9].

2.4. *In Vitro* and *ex Vivo* Autoradiography

Tg2576, dE9, and control mice aged 14 - 16 months were anaesthetized with isoflurane gas (1 mL per minute) and injected with 185 MBq/200 μL [^{18}F]-FDDNP through their lateral tail veins. Each group were killed by decapitation 30 min after injection. Their brains were immediately removed and frozen in powered dry ice. Sagittal sections of 20 μm cut and exposed to Kodak XAR film for 72 h.

2.5. MicroPET Imaging and Data Analysis

Mice were injected with about 18.5 MBq of [^{18}F]-FDDNP via the lateral tail vein. After distributed for 30 min, placed inside the microPET-R4® system (Concorde Microsystems, Knoxville, TN, USA) for tomographic imaging (10 min). AsiPro software (Concorde Microsystems) was used for the statistical analysis; a region of interest (ROI) was defined in each brain region.

2.6. Human Amyloid β(1 - 40) Enzyme-Linked Immunosorbent Assay (ELISA)

Mice were killed with carbon dioxide. Distinguishable regions (olfactory bulb, cortex, striatum, thalamus, hypothalamus, midbrain, cerebellum, Pons, and medulla) were transferred to polypropylene tubes and each sonicated sample was clarified for human amyloid β(1 - 40) ELISA Kit IBL code no. 27,713 (Immuno-Biological Laboratories Co., Ltd, Fujioka, Japan), according to the manufacturer's protocols.

3. Results and Discussion

[^{18}F]-FDDNP was developed in 2001 in Dr Barrio's laboratory at UCLA [10]. It has shown excellent results with AD in transgenic rats and patients *in vivo* and *in vitro* analyses [10] [11]. The lipophilic characteristic of [^{18}F]-FDDNP (1.93 ± 0.10) which was indicated high lipophilicity and suggested could penetrate the BBB.

The results of *in vitro* autoradiography and a competition assay (**Figure 1** and **Table 1**) demonstrate the high binding capacity and specificity of FDDNP in the Tg2576 transgenic mouse. In the Aβ-rich brain regions (hippocampus and frontal cortex), the dE9 mice also displayed significantly higher binding than the normal mice

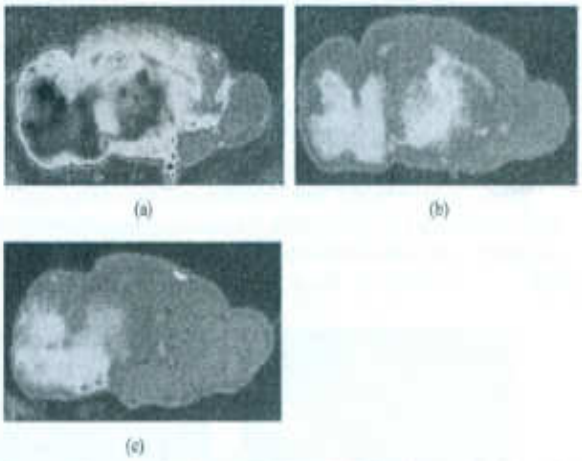

Figure 1. Brain autoradiography of transgenic mice ((a) Tg2576; (b) dE9) and normal mice (c) after incubation with [18F]-FDDNP.

Table 1. The binding of [^{18}F]-FDDNP, in different brain regions, derived from the brain autoradiograms shown in **Figure 1**, for the Tg2576 and dE9 transgenic mice and the competition assay groups treated with 20 or 200 μg of FDDNP carrier (n = 3, means ± SD).

Brain region	Tg2576 mice			dE9 mice			Normal mice		
	n.c.a.* [^{18}F]FDDNP	20 μg FDDNP carrier	200 μg FDDNP carrier	n.c.a. [^{18}F]FDDNP	200 μg FDDNP carrier	20 μg FDDNP carrier	n.c.a. [^{18}F]FDDNP	20 μg FDDNP carrier	200 μg FDDNP carrier
Cortex	109.79 ± 25.33	87.52 ± 22.48	33.92 ± 11.98$^{\#}$	27.41 ± 4.47†	6.63 ± 1.87$^{\#}$	4.77 ± 2.04$^{\#}$	7.19 ± 1.81	5.63 ± 0.73	2.44 ± 0.57
Hippocampus	49.15 ± 13.50†	34.16 ± 11.40	23.31 ± 9.30	8.71 ± 4.02	2.00 ± 1.08	1.65 ± 0.76	4.05 ± 1.04	4.74 ± 1.54	2.14 ± 1.08
Thalamus	73.07 ± 16.73†	28.94 ± 14.06$^{\#}$	17.75 ± 8.78$^{\#}$	9.73 ± 1.89	1.37 ± 0.39$^{\#}$	2.65 ± 1.02$^{\#}$	9.54 ± 1.98	4.52 ± 1.57$^{\#}$	10.33 ± 3.00
Hypothalamus	44.14 ± 15.02†	32.31 ± 8.02	19.44 ± 8.19$^{\#}$	8.25 ± 0.76	1.20 ± 0.84$^{\#}$	1.26 ± 0.78$^{\#}$	5.87 ± 1.20	4.35 ± 1.93	4.06 ± 1.27
Midbrain	39.39 ± 13.99†	28.51 ± 10.68	20.54 ± 0.76	6.72 ± 3.61	0.90 ± 0.34	3.82 ± 1.91	1.26 ± 1.14	8.36 ± 1.65$^{\#}$	2.43 ± 1.51
Pons	38.28 ± 15.53	24.97 ± 7.24	20.08 ± 11.06$^{\#}$	6.00 ± 2.04	1.87 ± 0.91$^{\#}$	0.02 ± 0.01$^{\#}$	5.43 ± 1.99	10.17 ± 4.98	3.50 ± 1.42
Medulla	38.61 ± 13.67†	28.57 ± 8.97	23.43 ± 13.96	8.33 ± 1.70	1.63 ± 1.01$^{\#}$	3.23 ± 1.20$^{\#}$	9.55 ± 2.83	1.49 ± 0.74	0.17 ± 0.10$^{\#}$
Cerebellum	115.50 ± 33.25	110.78 ± 27.45	48.93 ± 16.63	22.01 ± 13.54	12.36 ± 6.59	11.44 ± 4.24	22.70 ± 6.34	3.49 ± 1.59$^{\#}$	21.89 ± 12.11

* n.c.a: not-carrier-added. $^{\dagger}P < 0.05$, student's t test, for comparison within brain region and tracer, between carrier addition. $^{\#}P < 0.05$, for comparison within Tg2576 mice brain region between dE9 and normal mice. $^{\S}P < 0.05$, for comparison with brain region between dE9 and normal mice.

($p < 0.01$). Immunohistochemical staining of the Tg2576 mouse brains also identified high levels of Aβ protein in the hippocampus and frontal cortex (data not shown). We noted that in the Tg2576 mice, [^{18}F]-FDDNP accumulated strongly in the cerebellum, may be inferred that the overexpression of APP protein and the accumulation of Aβ plaques in the cerebellum [1] [4].

In the competition study, [^{18}F]-FDDNP binding was inhibited by co-incubation with the carrier (**Table 1**). More [^{18}F]-FDDNP accumulated in the Tg2576 brain than in the dE9 and normal mouse brains, and was not comprehensive among the brain regions.

Ex vivo autoradiography was also used to compare the binding of [^{18}F]-FDDNP to the Aβ-rich regions in the transgenic and normal mice (**Figure 2** and **Table 2**). The Tg2576 mice showed significant differences from the dE9 mice in the binding of [^{18}F]-FDDNP in the thalamus, midbrain, and medulla, and significant differences from the normal mice in the thalamus, midbrain, medulla, and cerebellum [3]. Although the data presented show only a few significant differences in the brain regions of the transgenic mice, our results are similar to those published by Kung *et al.* [12]. MicroPET imaging was performed 30 min after the injection of [^{18}F]-FDDNP (18.5 MBq). The signal quantified in the ROIs in these transverse sections compare with the reference baseline

indicated ratios of 0.84 - 1.00 relative to muscle in the Tg2576 mice (**Table 3**). When the radioactive signal of [^{18}F]-FDDNP was calculated relative to the same reference (muscle) in the dE9 transgenic mice, the ratios for different brain regions were 0.10 - 0.32 (**Table 3**). The specific binding ratios in whole brain regions showed greater accumulation of [^{18}F]-FDDNP in the Tg2576 mice than in the dE9 or normal mice (**Figure 3**). The immunoreactivity of human amyloid β(1 - 40) was quantified in the olfactory bulb, cortex, striatum, thalamus, hypothalamus, midbrain, cerebellum, pons, and medulla. A standard curve was constructed for human Aβ protein, ranging from 500 pg/mL to 7.813 pg/mL, and the linear standard curve equation was derived for continuous analysis (R2 = 0.995 - 0.998). In the Tg2576 mice, the amount of human β-amyloid in the whole brain (0.257 - 1.992 ng/mL) was significantly different from the amounts in the dE9 (0.085–0.567 ng/mL) and normal mouse brains (0.031 - 0.098 ng/mL) (**Table 4**). The present study suggests that [^{18}F]-FDDNP has excellent potential

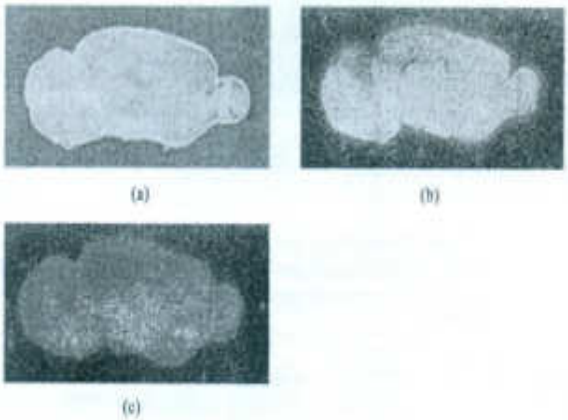

Figure 2. *Ex vivo* brain autoradiography of transgenic mice ((a) Tg2576; (b) dE9) and normal mice (c) 30 min after injection with 185 MBq/200 μL [18F]-FDDNP.

Table 2. The binding densities of [^{18}F]-FDDNP in different brain regions of the Tg2576 and dE9 transgenic mice and normal mice, derived from *ex vivo* brain autoradiograms (n = 3, mean ± SD).

	Tg2576	dE9	Normal mice
Cortex	48.21 ± 28.09	29.72 ± 15.83	10.93 ± 8.07
Hippocampus	48.48 ± 24.58	35.54 ± 16.64	13.97 ± 7.11
Thalamus	51.53 ± 19.16*	36.80 ± 17.91	12.54 ± 6.76#
Hypothalamus	41.36 ± 19.90	31.79 ± 13.82	10.94 ± 3.79
Midbrain	54.40 ± 16.05*	44.61 ± 15.06*	16.52 ± 8.16#
Pons	61.50 ± 25.09	35.74 ± 17.47	15.15 ± 6.48
Medulla	74.67 ± 24.26*	31.90 ± 9.31*	13.81 ± 6.55#
Cerebellum	54.28 ± 18.15	33.77 ± 7.06*	14.29 ± 6.87#

*$P < 0.05$, student's *t* test, for comparison within brain region and tracer, between Tg2576 and dE9 mice. †$P < 0.05$, for comparison within dE9 and normal mice. #$P < 0.05$, for comparison with Tg2576 and normal mice.

Table 3. Specific binding ratios for different brain regions (olfactory bulb, cortex, striatum, thalamus, and cerebellum) of the Tg2576 and dE9 transgenic mice and normal mice relative to that in muscle from the head region, derived from *in vivo* microPET images (n = 3, mean ± SD).

Specific binding ratio	Olfactory bulb	Cortex	Striatum	Thalamus	Cerebellum
Tg2576	0.90 ± 0.33*	0.91 ± 0.28*	1.00 ± 0.34*†	1.00 ± 0.27*†	0.84 ± 0.14*†
dE9	0.31 ± 0.17	0.22 ± 0.11	0.12 ± 0.07	0.10 ± 0.05	0.32 ± 0.11†
Normal mice	0.20 ± 0.14	0.19 ± 0.09	0.08 ± 0.02	0.07 ± 0.01	0.06 ± 0.02

*$P < 0.05$, student's *t* test, for comparison within brain region and tracer, between Tg2576 and dE9 mice. †$P < 0.05$, for comparison within dE9 and normal mice. #$P < 0.05$, for comparison with Tg2576 and normal mice.

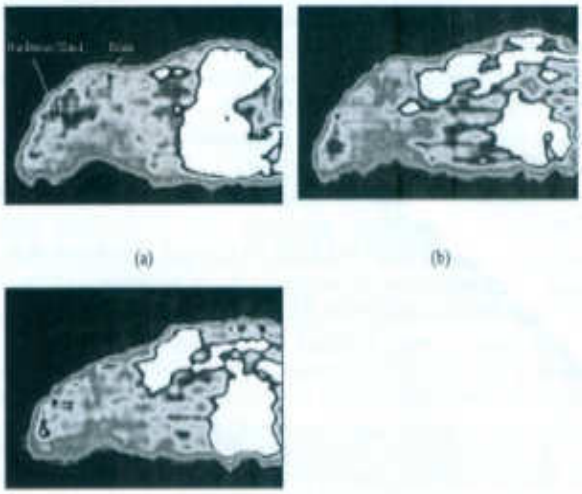

(a) (b)

(c)

Figure 3. *In vivo* microPET imaging of the accumulation of [18F]-FDDNP in brain sections 30 min post-injection into Tg2576 (a); dE9 (b); and normal mice (c).

Table 4. Levels of immunoreactivity for human amyloid β(1 - 40) in supernatants derived from different brain sections (olfactory bulb, cortex, striatum, thalamus, hypothalamus, midbrain, cerebellum, pons, and medulla) were quantified by ELISA using a human Aβ assay kit (n = 3, mean ± SD).

ng/ml	Tg2576	dE9	Normal mice
Olfactory bulb	1.992 ± 0.015*,+	0.171 ± 0.046*	0.031 ± 0.003
Cortex	1.984 ± 0.026*,+	0.567 ± 0.016	0.098 ± 0.005
Striatum	1.931 ± 0.007*,+	0.378 ± 0.086	0.031 ± 0.002
Thalamus	0.257 ± 0.017*	0.311 ± 0.018*	0.031 ± 0.001
Hypothalamus	0.386 ± 0.004*,+	0.293 ± 0.029*	0.030 ± 0.002
Midbrain	0.068 ± 0.003*,+	0.098 ± 0.008*	0.036 ± 0.001
Cerebellum	1.232 ± 0.018*,+	0.142 ± 0.067*	0.038 ± 0.001
Pons and medulla	0.078 ± 0.008*	0.085 ± 0.011*	0.039 ± 0.001

*$P < 0.05$, student's t test, for comparison within brain region and tracer, between Tg2576 and dE9 mice. +$P < 0.05$, for comparison within dE9 and normal mice. *$P < 0.05$, for comparison with Tg2576 and normal mice.

utility in Tg2576 mice, but not in dE9 mice, and that this correlates with the amounts of Aβ protein in their brains.

References

[1] Newberg, A.B., Wintering, N.A., Plössl, K., Hochold, J., Stabin, M.G., Watson, M., Skovronsky, D., Clark, C.M., Kung, M.P. and Kung, H.F. (2006) Safety, Biodistribution, and Dosimetry of 123I-IMPY: A Novel Amyloid Plaque-Imaging Agent for the Diagnosis of Alzheimer's Disease. *J Nucl Med.*, **47**, 748-754.

[2] Reiman, E.M., Uecker, A., Gonzalez-Lima, F., Minear, D., Chen, K., Callaway, N.L., Berndt, J.D. and Games, D. (2000) Tracking Alzheimer's Disease in Transgenic Mice Using Fluorodeoxyglucose Autoradiography. *Neuroreport*, **11**, 987-991. http://dx.doi.org/10.1097/00001756-200004070-00018

[3] Lee, C.W., Kung, M.P., Hou, C. and Kung, H.F. (2003) Dimethylamino-Fluorenes: Ligands for Detecting β-Amyloid Plaques in the Brain. *Nucl Med Biol.*, **30**, 573-580. http://dx.doi.org/10.1016/S0969-8051(03)00050-7

[4] Nakamura, S., Murayama, N., Noshita, T., Annoura, H. and Ohno, T. (2001) Progressive Brain Dysfunction Following

Intracerebroventricular Infusion of Beta1-42-Amyloid Peptide. *Brain Res.*, **912**, 128-136. http://dx.doi.org/10.1016/S0006-8993(01)02704-4

[5] Lockhart, A. (2006) Imaging Alzheimer's Disease Pathology: One Target, Many Ligands. *Drug Discov Today*, **11**, 1093-1099. http://dx.doi.org/10.1016/j.drudis.2006.10.008

[6] Routtenberg, A. (1997) Measuring Memory in a Mouse Model of Alzheimer's Disease. *Science*, **277**, 839-841. http://dx.doi.org/10.1126/science.277.5327.839

[7] Barrios, J.R., Kepea, V., Satyamurthy, N., Huang, S.C. and Gary, W. (2006) Brain Pathology and Neuronal Losses in the Living Brain of Alzheimer's Patients. *Int Congr Ser.*, **1290**, 150-155. http://dx.doi.org/10.1016/j.ics.2005.11.102

[8] Giovannelli, L., Casamenti, F., Scali, C., Bartolini, L. and Pepeu, G. (1995) Differential Effects of Amyloid Peptides β-(1-40) and β-(25-35) Injections into the Rat Nucleus Basalis. *Neuroscience*, **66**, 781-792. http://dx.doi.org/10.1016/0306-4522(94)00610-H

[9] Liu, J., Kepe, V., Zabjek, A., Petric, A., Padgett, H.C., Satyamurthy, N. and Barrio, J.R. (2007) High-Yield, Automated Radiosynthesis of 2-(1-{6-[(2-[18F]Fluoroethyl)(methyl)amino]-2-naphthyl}ethylidene)malononitrile ([18F]FDDNP) Ready for Animal or Human Administration. *Mol Imaging Biol.*, **9**, 6-16. http://dx.doi.org/10.1007/s11307-006-0061-4

[10] Agdeppa, E.D., Kepe, V., Liu, J., Flores-Torres, S., Satyamurthy, N., Petric, A., Cole, G.M., Small, G.W., Huang, S.C. and Barrio, J.R. (2001) Binding Characteristics of Radiofluorinated 6-Dialkylamino-2-Naphthylethylidene Derivatives as Positron Emission Tomography Imaging Probes for β-Amyloid Plaques in Alzheimer's Disease. *J Neurosci.*, **21**, RC189.

[11] Agdeppa, E.D., Kepe, V., Liu, J., Small, G.W., Huang, S.C., Petric, A., Satyamurthy, N. and Barrio, J.R. (2003) 2-Dialkylamino-6-acylmalononitrile Substituted Naphthalenes (DDNP Analogs): Novel Diagnostic and Therapeutic Tools in Alzheimer's Disease. *Mol Imaging Biol.*, **5**, 404-417. http://dx.doi.org/10.1016/j.mibio.2003.09.010

[12] Kung, H.F., Kung, M.P., Zhuang, Z.P., Hou, C., Lee, C.W., Plössl, K., Zhuang, B., Skovronsky, D.M., Lee, V.M. and Trojanowski, J.Q. (2003) Iodinated Tracers for Imaging Amyloid Plaques in the Brain. *Mol Imaging Biol.*, **5**, 418-426. http://dx.doi.org/10.1016/j.mibio.2003.09.003

5. 會議照片